nature climate change

SUPPLEMENTARY INFORMATION

DOI: 10.1038/NCLIMATE1514

Extinction debt of high-mountain plants under twenty-first-century climate change

Stefan Dullinger[1,2*], Andreas Gattringer[1], Wilfried Thuiller[3], Dietmar Moser[1], Niklaus E. Zimmermann[4], Antoine Guisan[5], Wolfgang Willner[1], Christoph Plutzar[1,6], Michael Leitner[7,8], Thomas Mang[1,2], Marco Caccianiga[9], Thomas Dirnböck[10], Siegrun Ertl[2], Anton Fischer[11], Jonathan Lenoir[12,13], Jens-Christian Svenning[12], Achilleas Psomas[4], Dirk R. Schmatz[4], Urban Silc[14], Pascal Vittoz[5], & Karl Hülber[1]

April 02, 2012

[1] Vienna Institute for Nature Conservation and Analyses, Giessergasse 6/7, A-1090 Vienna, Austria
[2] Faculty Centre of Biodiversity, University of Vienna, Rennweg 14, A-1030 Vienna, Austria
[3] Université Grenoble I, CNRS, Laboratoire d'Ecologie Alpine, UMR 5553, BP 53, 38041 Grenoble Cedex 9, France
[4] Landscape Dynamics Unit, Swiss Federal Research Institute WSL, CH-8903 Birmensdorf, Switzerland
[5] Department of Ecology and Evolution, University of Lausanne, Bâtiment Biophore, CH-1015 Lausanne, Switzerland
[6] Institute of Social Ecology Vienna (SEC), Alpen-Adria-University, Schottenfeldgasse 29, A-1070 Vienna, Austria
[7] Faculty of Physics, University of Vienna, Strudlhofgasse 4, A-1090 Vienna, Austria
[8] FRM II, Technical University of Munich, Lichtenbergstraße 1, 85747 Garching, Germany
[9] Department of Biology, Università degli Studi di Milano, Via Celoria 26, I-20133 Milan, Italy
[10] Environment Agency Austria, Department for Ecosystem Research & Monitoring, Spittelauer Lände 5, 1090 Vienna, Austria
[11] Geobotany, Center of Life and Food Sciences, Technische Universität München, Hans-Carl-von-Carlowitz-Platz 2, D - 85354 Freising
[12] Ecoinformatics & Biodiversity Group, Department of Bioscience, Aarhus University, Ny Munkegade 114, DK-8000 Aarhus, Denmark
[13] Ecologie et Dynamique des Systèmes Anthropisés (EA4698), Université de Picardie Jules Verne, 1 rue des Louvels, F-80037 Amiens Cedex, France
[14] Institute of Biology Zrc Sazu, Novi trg 2, SI-1000 Ljubljana, Slovenia

* corresponding author: stefan.dullinger@univie.ac.at

The Supplementary Information contains the Supplementary Methods, the Supplementary Figures S1–S3, and a Supplementary Table 1.

Supplementary Methods

All modelling was done on a two-dimensional grid representing the Alps at a 100 m spatial grain.

Current and future climatic data

Current climate was mapped as 100 m raster data, downscaled from 1 km Worldclim climate grids available online[1]. Worldclim provides long-term monthly climate averages for the period of 1950–2000 for precipitation and minimum, average and maximum temperature and a series of nineteen bioclimatic variables directly derived from the monthly grids[2]. We first downscaled monthly base maps to a spatial resolution of 100 m, in order to better represent the topographic variation of climate in our study area. In a second step we used these downscaled temperature and precipitation grids to re-generate maps of five bioclimatic variables which (1) have an obvious impact on plant life in mountain environments; and (2) showed some independent variation across the study area ($r < 0.9$ throughout, and mostly < 0.75): the minimum temperature of the coldest quarter of the year (bio6), the temperature annual range (bio7), the mean temperature of the warmest quarter (bio10), the precipitation sum of the warmest (bio17), and coldest quarters (bio18).

The downscaling procedure can be summarized as follows: at the 1 km spatial resolution, we analysed the dependency of precipitation and temperature on elevation by means of linear regressions in circular moving windows of 15 and 25 km radius, respectively. We chose smaller moving windows for precipitation, because of the better fit in cross-validation exercises. By doing so, we extracted the hidden lapse rates and ’0 m above sea level‘ temperature and precipitation intercepts inherent in the Worldclim maps. We stored lapse rates and intercepts to the centre cell of each window position and then spatially interpolated these regression parameters to a 100 m resolution by means of inverse distance-weighted interpolation. Finally, the interpolated regression parameters were applied for back conversion

to climate maps using a 100 m digital elevation model, which was aggregated from the 90 m SRTM DEM[3] version 4.0 by means of the AGGREGATE command in ArcGrid. In summary, this procedure allowed us to first extract the hidden regression parameters of the Wordclim maps, and then to spatially scale them to the resolution of 100 m. The same approach to statistical downscaling of climatic parameters has already been used in several earlier studies[4,5,6,7].

Since we used projections of (future) climates that were only available as a time series starting in 1961, we had to correct the 1950–2000 monthly averages to 1961–2000 monthly baselines. We used the CRU TS1.2 monthly temperature and precipitation time series[8] with a spatial resolution of 10' (~18 km) in order to generate monthly difference maps for the two different baselines, namely the 1950–2000 baseline from Worldclim and the 1961–2000 baseline of modelled future climates. These anomaly maps were then scaled from the 10' to a 1 km spatial resolution by means of inverse-distance weighted interpolation, and added to the Worldclim maps in order to convert these to 1961–2000 baselines. These baselines were imported from GIS raster formats into the NetCDF format.

Projections of monthly temperature and precipitation series for the 2001 to 2100 time span were taken form simulations that the Max Planck Institute (MPI) has generated based on a regional circulation model (RCM). Specifically, we used the climate limited-area modelling community (CLM) model runs[9], which were fed by output from the ECHAM5 general circulation model (GCM) for the A1B scenario. This output is available as a 1961–2100 daily or monthly data series in NetCDF format at a 20' (~36 km) spatial resolution, and can be downloaded from the CERA world data centre for climate in Hamburg (http://cera-www.dkrz.de/CERA).

We chose this climate model because it projects, on average, an intermediate level of both increasing temperatures and decreasing precipitation over Europe as compared to a range of RCM simulations carried out by the ENSEMBLES FP6 EU project. In Fig. M1 we illustrate

this intermediate position for both summer (April-September) and winter (October-March) anomalies compared to a 1950–2000 reference period of seasonal means. Anomalies in temperature are given in absolute numbers (°C), while anomalies in precipitation are reported as % change relative to the baseline period.

For this newer generation of RCMs provided by the ENSEMBLES model system, the A1B scenario was always calculated, while other scenarios were not consistently generated. In addition, the A1B scenario is intermediate compared to the more extreme A2 on the one hand, and the milder B1/B2 scenarios. We therefore used the A1B scenario output from the CLM model.

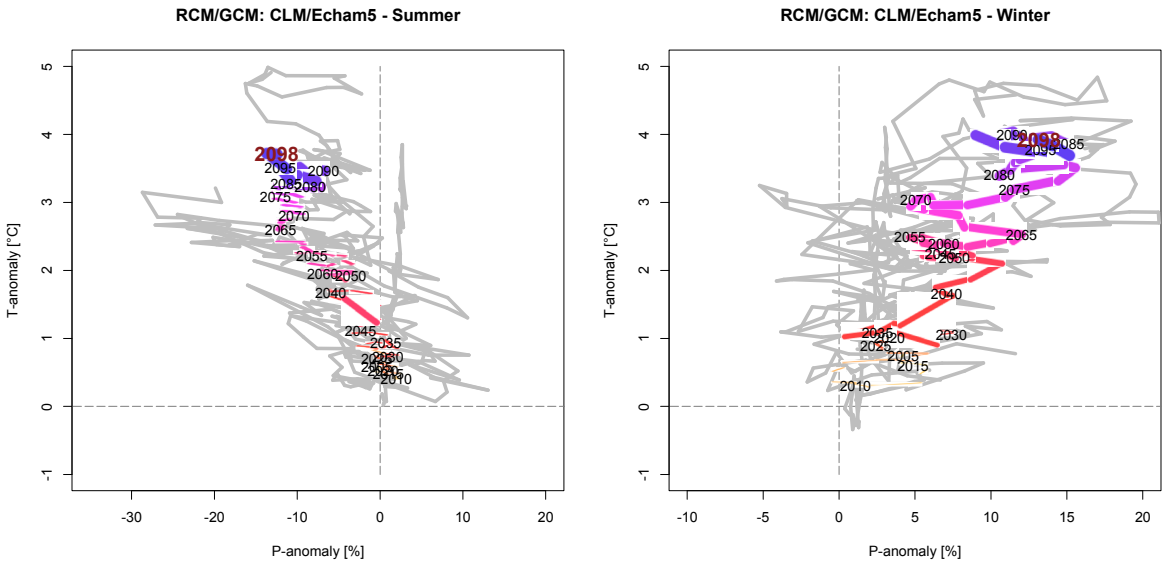

Fig. M1 Anomalies in temperature (°C) and precipitation (% change) simulated by the CLM/ECHAM5 model run (in color) for the IPCC A1B scenario compared to 5 other regional circulation models originating from the regional climate ensemble prediction system for climate change in Europe (FP6 ENSEMBLES). The lines represent the climate development in Europe according to six RCMs, among which the CLM/ECHAM5 model is highlighted in color. The 21st century starts with yellow colors around 2000, and ends with blue-magenta colors in the year 2098, while every 5th year is labelled. Each dot of the line represents a 5-year seasonal mean. The following 5 additional RCM/GCM pairs are drawn in grey for the A1B scenario: HadRM3q0/HadRM3, Racmo/ECHAM5, Hirham/Arpège, RCA30/CCSM3, and RCA30/ECHAM5.

We downloaded the monthly averages, and then calculated monthly anomalies for temperature (min, average, max) and precipitation (sum) against a 1961–2000 monthly mean

of the same CLM simulation output. By doing so we hence calculated the changing climate series relative to the same baseline time span available from Worldclim[1]. Anomalies for temperature were expressed as absolute differences, while precipitation anomalies were calculated as relative differences. These anomalies were then scaled in a first step to a 1 km, and in a second step to a 100 m spatial resolution. Next we added (temperatures) or multiplied (precipitation) the anomalies at the 100 m spatial resolution with the downscaled 100 m climate maps in order to generate monthly climate time series for our study area. Finally, we exported the climate maps to a GIS, meaning that all calculation steps from the raw CLM data to the 1 km climate anomalies were performed in a NetCDF environment using the climate data operators (cdo) tool of the Max-Planck institute of meteorology (https://code.zmaw.de/projects/cdo). By this we had derived a time series of future climate data at a 100 m spatial and a monthly temporal resolution. This is the same approach used in earlier studies[4,5,6,7] .

Finally, we re-calculated the five bioclimatic variables for the full time series 2001–2100 and then smoothed these series by a nine-years moving average to measure climatic suitability of sites by mid-term climatic conditions rather than by annual fluctuations. For reasons of computing time, the species' occurrence probabilities (see below) were projected onto the climatic surfaces of every tenth year only (Fig. M2).

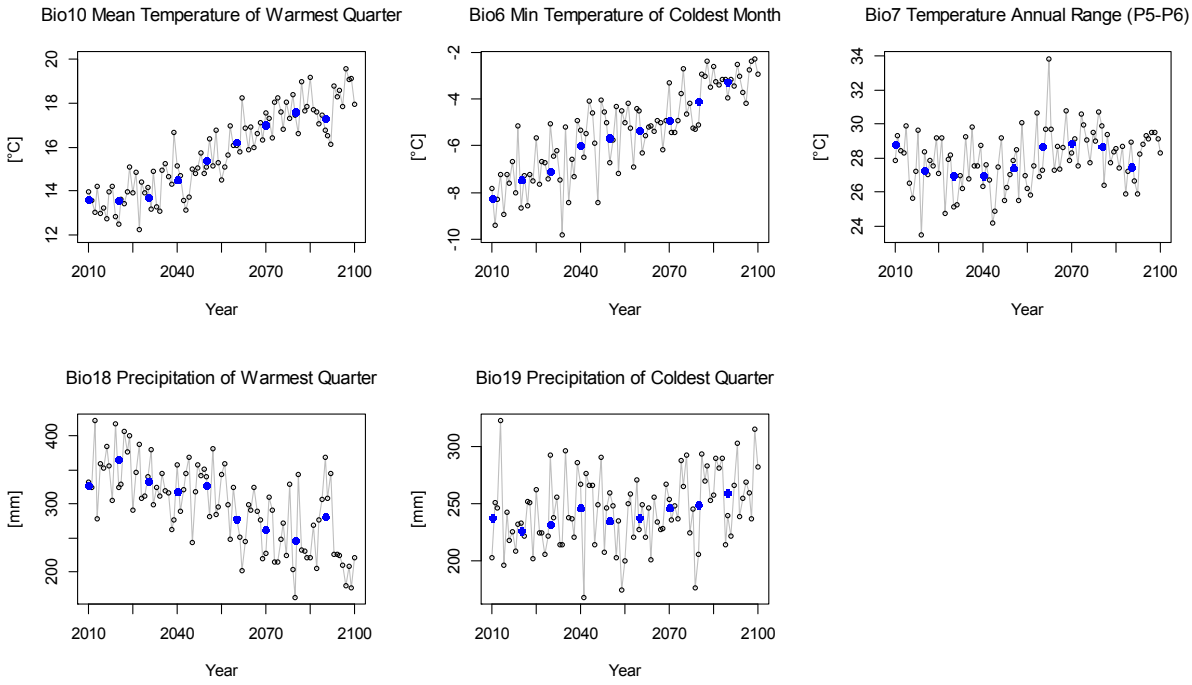

Fig. M2 The grey lines represent annual time series of the five bioclimatic variables derived from predictions of mean monthly temperatures and precipitation sums according to the CLM/ECHAM5 model run for the IPCC A1B scenario[9]. The blue dots symbolise values of every 10th year (2010, 2020, 2030, ..., 2100) derived from smoothing annual series by 9-year running means. These 10th-year values were used to project niche-based occurrence probabilities of the study species.

Geological data

Using information from the European Soil Database[10] we calculated the percentage area of Soil Typological Units (STU) having a calcareous dominant parent material for every Soil Mapping Unit (SMU) within the borders of the Alpine chain (Fig. M3). For the Austrian part of the Alps, a fine-scaled map of substrate units was available[11] which we used to compute the area of calcareous substrates within grid cells of 5' longitude × 3' latitude in order to get information compatible to that derived from the European Soil Database.

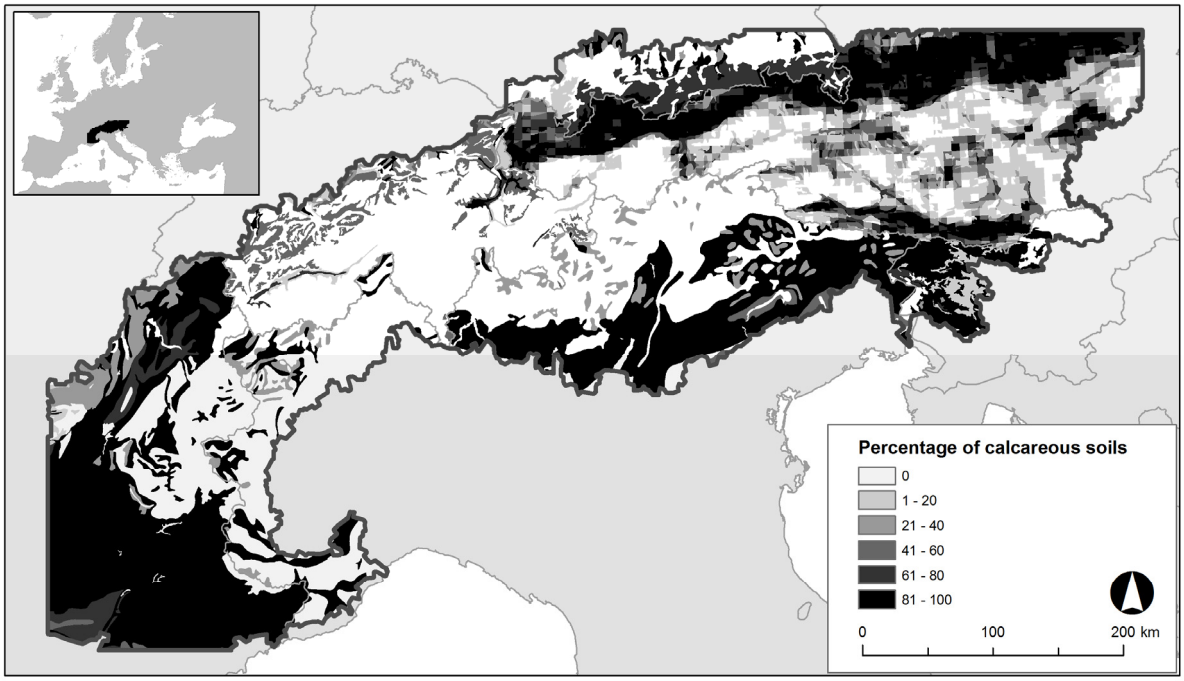

Fig. M3 Incidence of calcareous substrates in the Alps. For France, Switzerland, Germany, Italy, and Slovenia, the map is based on the Soil Mapping Units of the European Soil Database[10]; for Austria on cells of a regular 5' longitude × 3' latitude raster.

Vegetation plot data

We compiled 14,040 localized plot data (between 1 and 100 m²) from subalpine and alpine non-forest vegetation of the Alps from published[12] and own, unpublished databases (Fig. M4).

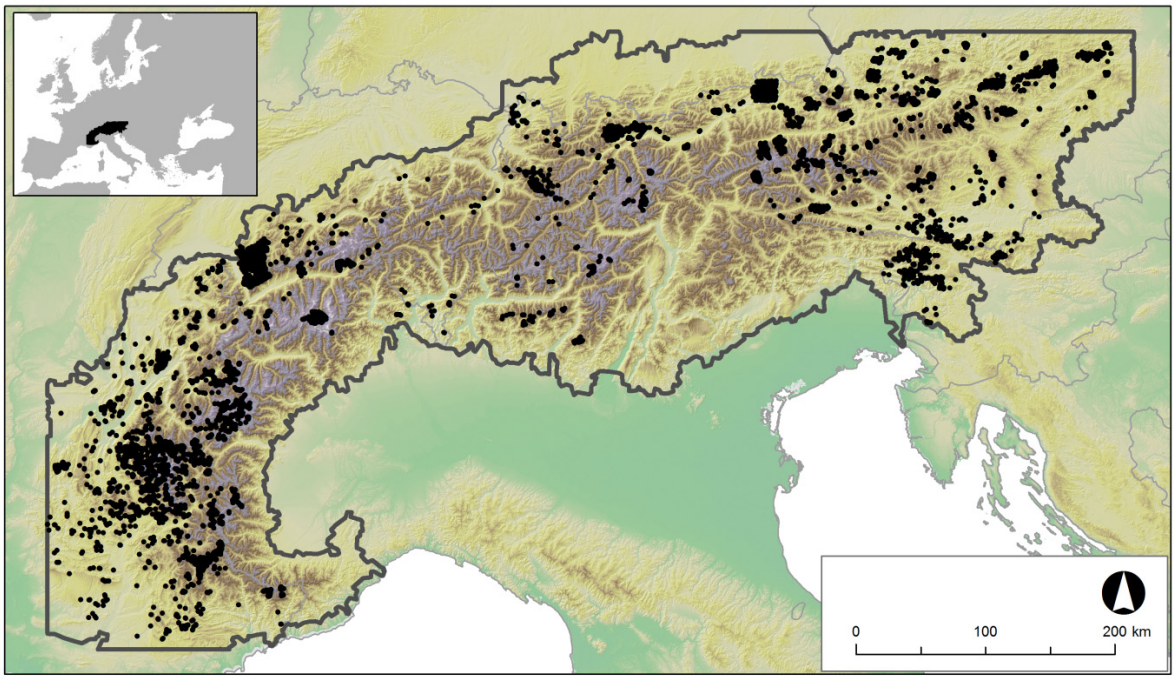

Fig. M4 Distribution of vegetation plots (black dots) used for calibrating niche-based models. The bold line represents the border of the study area, the bright grey lines are country borders.

These plot data did not cover the entire Alps homogeneously, but had low coverage in the Italian Alps. We hence tested their representativeness for the whole area of the subalpine and alpine belts of the Alps in terms of the five bioclimatic variables used for modelling by comparing variable values of the vegetation plots (i.e. the 100 m × 100 m raster cells including a vegetation plot) with 500 random samples of the same size (= 14,040) drawn from the total set of raster cells covering the Alpine area at altitudes > 1,400 m a.s.l.. Median values and value distributions of empirical and randomly sampled sites were quite similar for each of the five bioclimatic variables (Fig. M5) as well as in five-dimensional bioclimatic space (Fig. M6).

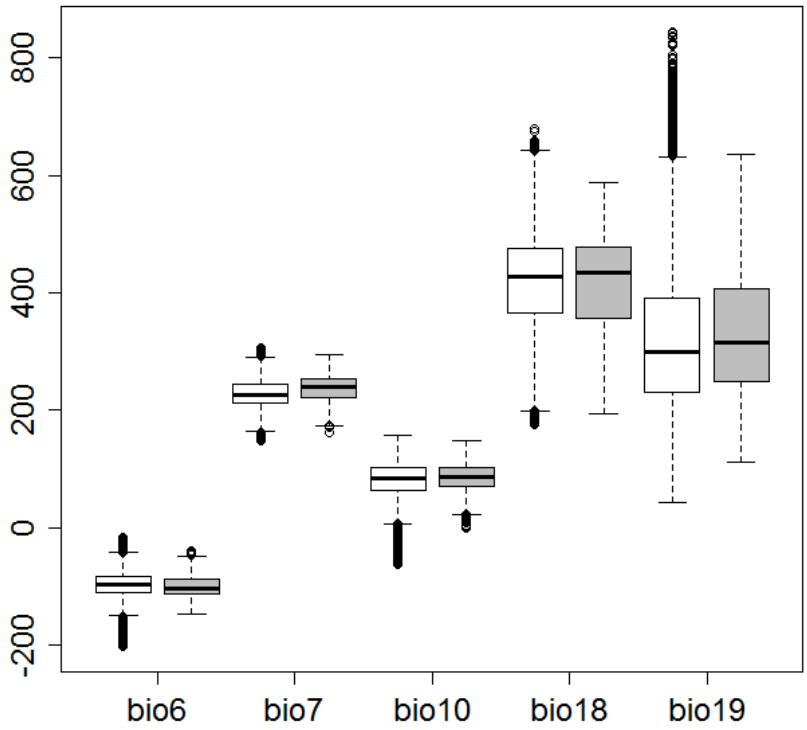

Fig. M5 Value distributions (boxplots) of the five bioclimatic variables[1] in the niche-based models in 500 random sets of 14,040 100 m × 100 m cells from the study area above 1,400 m a.s.l. (white) and in the empirical set of 14,040 100 m × 100 m cells in which the vegetation plots used for fitting niche models are located (grey). Temperature variables (bio6, bio7, and bio10) are in 1/10°C and precipitation variables (bio18 and bio19) are in mm/quarter of the year.

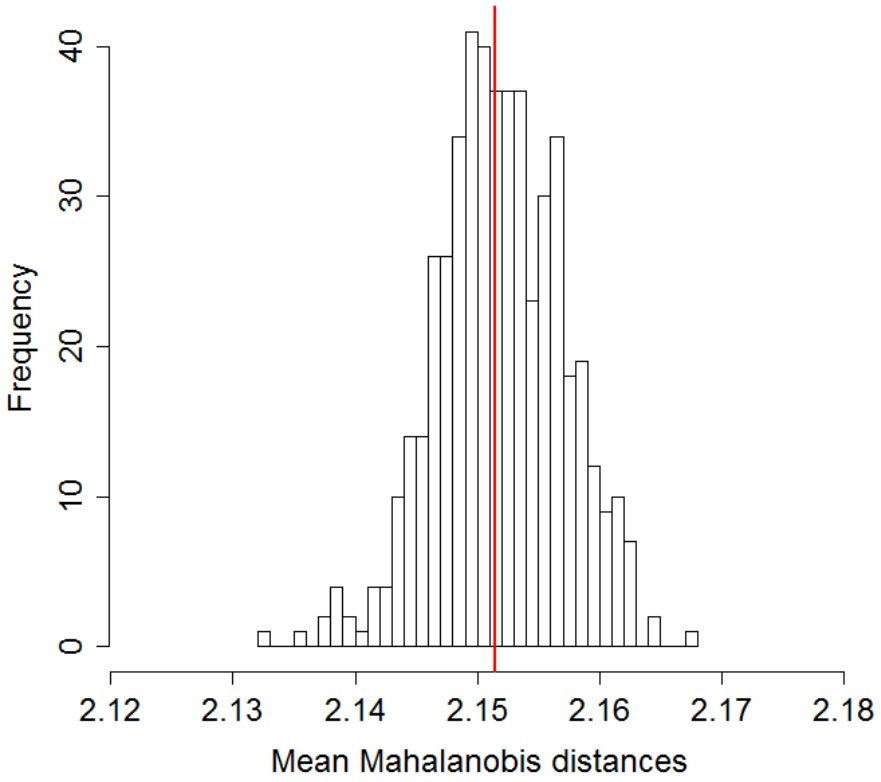

Fig. M6 Histogram of the mean Mahalanobis distance of 500 random sets of 14,040 100 m × 100 m cells (drawn from the study area above 1400 m a.s.l.) to the centroid of all raster cells of the study area. The five dimensions are the five bioclimatic variables used for niche-based models (see Fig. M5). The red line symbolizes the respective distance for the empirical set of 14,040 100 m × 100 m cells in which the vegetation plots used for fitting niche models are located. The covariance matrix used for the calculation of the Mahalanobis distance was based on all raster cells.

Niche-based models

For each of the 150 species, presence and absence data from the vegetation plots were related to the set of bioclimatic (WorldClim baseline data 1961–2000) and soil variables using three different techniques implemented in R and available in the BIOMOD library[13], namely generalized additive models (GAM), boosted regression trees (BRT) and random forests (RF). The three selected techniques are known to be of very high predictive accuracy and computationally efficient[14]. We did not use more techniques due to the large extent of the study system.

GAMs were calibrated using a maximum of four degrees of smoothing. No interactions were allowed. BRTs were calibrated using a maximum of 3,000 trees, an interaction depth of 7 and a shrinkage of 0.001. The optimal number of trees was selected using a 5-fold cross-validation procedure internal to the function. Random forests were run with the default parameters of the original function with a maximum number of trees set to 750.

For each species and modelling technique, the original data were randomly divided into two sub-parts, one for calibrating the models (80%) and one for evaluating them (remaining 20%) using the True Skill Statistic[15] (TSS). This process was repeated 5 times to make sure that the estimated predictive accuracy was not influenced by the random partitioning. TSS takes into account both omission and commission errors, and success as a result of random guessing, and ranges from −1 to +1, where +1 indicates perfect agreement and values of zero or less indicate a performance no better than random. If a modelling technique failed to reach a mean TSS > 0.6 on the evaluation data, this technique was not retained for this particular species to make the final projection under current and future conditions.

For each species, we projected the probability of occurrence within each 100 m × 100 m cell of the study system under both current and future climatic conditions as a weighted sum of occurrence-probability projections made by the three modelling techniques[16]. The weighting scheme was proportional to the TSS statistics for each modelling technique (i.e. the techniques that delivered the most accurate models had the highest weights). As already mentioned, projections under future climatic conditions were restricted to every 10^{th} year (2010, 2020, 2030, …, 2100) for reasons of feasibility in terms of computing time. Occurrence probabilities for the intermediate years were linearly interpolated between these 10^{th} year values.

Demographic models

The three main life history stages distinguished in the hybrid model (seeds, juveniles and adults) were further sub-divided into sub-stages according to the life history characteristics of the species (age of maturity and seed persistence). Year-to-year transitions among these stages drive the local demography. For each cell within each time step, the model:

- partitions the seed yield (either of local origin or arriving from other cells) to seedlings (i.e. first-year juveniles or adults in the case of annuals) and the seed bank.

- re-calculates the number of seeds in each seed age class of the seed bank according to species-specific seed persistence and germination rates.

- re-calculates the number of juveniles in each juvenile sub-stage (= age class in years) according to the specific germination and juvenile survival rates, and durations of pre-maturity.

- re-calculates the number of adults according to juvenile survival (from the eldest prematurity age to the earliest adult age), adult mortality and clonal growth rates.

- calculates the number of seeds produced by the local adult population according to the respective flowering frequency and seed yield rates.

The rates which determine the transition of individuals or shoots among different stages or sub-stages, or the stasis within the same (sub-)stage (seed survival in the seed bank, germination, juvenile survival, clonal growth and mortality, fecundity), are modelled as both species and, with the exception of seed bank persistence, habitat dependent. We account for this double dependency by making species-specific rates a function of site suitability, with the latter measured by the occurrence probability projections of the niche-based models. In particular, we assume that for a given species *s* this relationship follows a sigmoid function given by

$$rate_{s,i,t} = \frac{1}{1 + e^{a(ST_s - NMpr_{s,i,t})}} \cdot maxrate_s \cdot f(N_{s,i,t}), \quad (1)$$

where $NMpr_{s,i,t}$ is the occurrence probability of species *s* at site *i* as predicted by the niche-based model for time (= year) *t*, *a* is a parameter that determines the slope of the logistic curve, $maxrate_s$ is the species' maximum rate under well-suited environmental conditions (cf. Supplementary Table 1), and $f(N_{i,s,t})$ is an optional functional form, used for introducing density dependence (see below). ST_s is the prevalence of the species in the data set used to calibrate the niche model, a threshold commonly used to translate probability-scaled predictions of niche-based models into binary presence-absence forecasts[17]. Using ST_s as specified in equation (1) ecologically implies that the given rate reaches half of the species-specific maximum (= the inflection point of the sigmoid function) at sites classified as marginally suitable for long-term species persistence by the niche models. Modifications of equation (1) may shift this point where half of the maximum rate is realized (see below). The parameter *a* was set to 15 by default as this value produced a reasonable form of the logistic function over a broad range of *ST* values. All functions are implemented such that they are bounded between [0, $maxrate_s$].

In addition to *ST*, the model uses a further threshold of site suitability below which all demographic rates drop to 0. For each species separately, we defined this threshold as the lowest occurrence probability that the niche-based model predicts for a site currently occupied by the respective species according to the calibration data, i.e. the 14,040 vegetation plots.

We accounted for density dependence in the following rates: germination, juvenile survival, and clonal growth. Density dependence in equation (1) was implemented through the factor $f(N_{s,i,t})$:

$$f(N_{s,i,t}) = \frac{C_{s,i,t} - N_{s,i,t}}{C_{s,i,t}}, \quad (2)$$

where $C_{s,i,t}$ is the carrying capacity of species s at site i and time t and $N_{s,i,t}$ is the actual local population size (number of adult individuals or shoots) of the respective species.

Carrying capacity is defined as the maximum number of adult individuals per site. It was derived from the species-specific size of an individual in relation to the size of the site (100 m × 100 m) and the maximum proportion of the available space that a species can occupy in a cell under suitable conditions (Supplementary Table 1). The specific carrying capacity of a species at a particular site and year is related to site suitability, i.e. the species' local occurrence probability as predicted by the niche-based model, in the same way as the demographic rates.

Fecundity, i.e., the number of seeds produced per average adult individual in a cell's population per year, is modelled as the product of flowering frequency (proportion of individuals flowering) and seed yield per individual (Supplementary Table 1). Flowering frequency was related to site suitability without accounting for density dependence (i.e. $f(N_{s,i,t}) = 1$). Seed yield was constrained to sites with a predicted occurrence probability $\geq ST$, i.e. we forced the sigmoid to drop to 0 at its inflection point. This guaranteed that seeds can germinate and grow to adults, though with low rates, at sites with suitability values $< ST$, but that these populations actually represent sinks which are unable to produce 'emigrants' and hence cannot act as stepping stones of migration.

Adult mortality was integrated with clonal growth to a single compound rate which describes the rate by which the adult population of a site changes from one year to the next (apart from adult recruitment from the juvenile cohorts). This compound rate *clgr* simultaneously accounts for (a) site suitability, (b) density dependence, and (c) age-specific mortality, by using the following equation:

$$clgr_{s,i,t} = \min\left(\begin{array}{l} 1+\left(\left(maxclgr_s - 1\right)\left(\dfrac{C_{s,i,t} - N_{s,i,t}}{C_{s,i,t}}\right)\right), \\ \dfrac{1}{1+e^{a(ST_s - NMpr_{s,i,t}}}\left(2+\left(\dfrac{maxclgr_s}{maxage_s} - ageofmaturity_s\right)\right) \end{array}\right) \quad (3)$$
$$-\left(\frac{1}{maxage_s - ageofmaturity_s}\right)$$

where the factor $(2 + [(maxclgr_s/maxage_s) - ageofmaturity_s]$ guarantees that $clgr_{s,i,t}$ reaches 1 at ST_s.

Hence, for a clonal species *s* at site *i* and time *t*, the adult population increases if the niche model predicts an occurrence probability $NMpr_{s,i,t} > ST_s$, it remains constant if $NMpr_{s,i,t} = ST_s$, and it decreases if $NMpr_{s,i,t} < ST_s$. At the latter sites, populations can hence, in the long run, only survive if seed input from abroad is high enough to compensate for population shrinkage because own recruitment from seeds is inhibited (fecundity = 0 where occurrence probability < *ST*, see above), similar to the rescue effect in metapopulation models[18]. The density-dependent component is implemented in the same way as for germination and juvenile survival, i.e. by using $f(N_{s,i,t})$ as defined in eq. (2) as a shrinkage factor to the maximum achievable clonal growth rate. This guarantees that the clonal growth rate decreases with population size. It additionally introduces density-dependent mortality as the clonal growth rate drops below 1 even at suitable sites if the number of individuals transcends the carrying capacity. Finally, we introduce an additional background mortality rate as the inverse of the genet's life time (minus the duration of the juvenile stage; last term in eq. (3).

Seed bank persistence is the only rate which is not modelled as site specific because habitat requirements of seeds likely do not match those of other life stages. By default, it is hence assumed that the number of seeds surviving from one year to the next is linearly decreasing to zero at the species-specific maximum persistence.

For each time step and site, individual/shoot, or seed numbers in each stage or sub-stage class were varied stochastically by drawing random numbers from a Poisson distribution. The rate

parameter of the Poisson distribution was set to the expected number of individuals in the respective stage or sub-stage as calculated by the above specified transition rates

Dispersal models

The seeds of most species are polychorous[19,20]. We accounted for this fact by distributing the seed yield according to a wind and two animal dispersal kernels.

Wind dispersal

Wind dispersal kernels were parameterized using the mechanistically based analytical WALD model[21]. Species-specific parameter values (seed release height, seed terminal velocity) needed were derived from the literature, databases or own measurements (Supplementary Table 1). Vegetation height surrounding fruiting individuals was set to three alternative values depending on the vegetation type a species is typically occurring in (Supplementary Table 1). Wind speed data were taken from a 9-year (2000–2008) series of average wind speeds of 10 min intervals during the seed shedding seasons (July–December) measured in a weather station of the central Austrian Alps (Mt. Sonnblick, 12°57'29' E, 47°03'16'' N, 3105 m a.s.l..). Wind speeds were corrected from measurement height (10 m) to seed release height by integration over a logarithmic wind profile following Skarpaas & Shea[22]. The necessary parameters were set to K = 0.4 (von Kármán constant[21]), d = 0.7 · surrounding vegetation height, and z_0 = 0.1 · surrounding vegetation height (surface roughness parameters[22,23]). Friction velocity and the instability paramter σ were calculated using equations (2) and (4) in Skarpaas & Shea[22] with Co = 3.125 (Kolmogorov constant). Geographical and topographical variation in wind speed distribution patterns were not accounted for to keep model complexity at a feasible level.

The WALD model provides a probability density of dispersal distances for specified wind conditions. To arrive at an 'average' dispersal kernel across several seed shedding seasons, we

integrated the WALD kernel over the empirical density of wind speed distribution[22] across the nine seed shedding seasons at the Mt. Sonnblick station.

Animal dispersal

Animal dispersal kernels were modelled by combining simulations of animal vector movements with estimates of seed detachment and gut survival rates. We focused on chamois (*Rupicapra rupicapra* L.) as an animal vector in these models, as chamois are the most frequent large mammal in the study area and hence probably the most efficient long-distance dispersal agent.

The core of animal dispersal models is a simulation routine that creates animal movement patterns as a mixture of correlated random walks[24], i.e. a combination of random walks with step lengths, movement velocities and turning angles varying among different activity phases of the animal such as grazing, ruminating, or sleeping. Differentiation of states, probability distributions of state durations and among-state transitions as well as state-specific parameter values of the above movement components were taken from the literature, in particular from the telemetric data reported in Frankhauser & Enggist[25]. Essentially, we created a time series of activity states and then simulated random walks based on a constant step duration of 3 minutes (or shorter, if the activity state was simulated to change earlier). Movement velocities during these steps as well as step-connecting turning angles were randomly drawn from the activity-dependent distributions of these parameters documented in Frankhauser & Enggist[25]. In accordance with the literature, the created movement patterns mostly remained within a home range of ~ 1 km² [26,27]) but include occasional home range movement walks of up to 5 km length[25].

During the simulated random walks, we assumed that seeds were attached to the animal at a random starting location and detached following species-specific detachment rates. These detachment rates were modelled as dependent on the species' seed mass and seed surface

structure according to a regression equation published by Römermann *et al.*[28]. The species-specific parameter values (seed mass, seed surface structure) needed were derived from the literature, databases or own measurements (Supplementary Table 1). As Römermann *et al.*[28] have published separate functions for either sheep or cattle furs, but none for chamois, we calculated both rates and took the average in our calculations. Dispersal kernels were finally calculated as empirical probability densities of the distances between the recorded attachment and detachment locations in each of 10,000 random walks per plant species.

Endozoochoric dispersal kernels were constructed in the same way as exozoochoric ones assuming that gut passage times (the time between seed uptake and defecation) follows a normal probability density function with a mean of 30 hours and a standard deviation of 5 hours. These mean and variance parameters are intermediate between the values reported in the literature for roe deer[29] and red deer[30] and were considered constant across all plant species. The resulting empirical dispersal distance distribution was then weighted by the species-specific gut survival probabilities which were calculated from seed weights based on a regression equation parameterized by Moussie[31].

Compound dispersal kernel

Although the different vectors probably contribute to the seed dispersal of most real populations, no information on their quantitative shares is available in the literature. Similar as with those demographic parameters for which information is sparse (Supplementary Table 1) we hence used a low and high parameter set representing contrasting assumptions about the frequency of longer dispersal distances: the 'low' parameter set assumed that 0.1% – 0.5% of the annual seed yield of a site's population are distributed by the more fat-tailed zoochorous vectors[32]; the 'high' parameter set assumed a one order of magnitude higher contribution of exo- and endozoochorous dispersal pathways (1% – 5%). The actual mixture of component kernels was determined separately for each population and year by (uniformly distributed)

random draws from these two alternative ranges of proportions. The remaining percentage of the seed yield was distributed according to the wind kernels.

As with demographic models, the number of seeds arriving in each recipient site (100 m × 100 m cell) of the study system was stochastically modified by drawing random numbers from a Poisson distribution with the expected value defined by the summed contributions from all existing populations as calculated by their compound dispersal kernels.

Hybrid model program flow

The hybrid model simulated local population dynamics driven by changing local site suitability via the sigmoid functions and distributed the resulting local seed yields according to the dispersal kernels, potentially giving rise to the colonization of new sites. The simulation time step was annual.

To link site suitability values under 'current' climatic conditions (average of the period 1961–2000) with those under the climate change scenario we assumed that data on these current conditions are representative for the year 1975 and linearly interpolated projected occurrence probabilities values between this '1975' and the projections for 2020. We then derived initial species distributions for the year 1990 by defining all sites with a 1990-occurrence probability value greater than the species' prevalence in the calibration data set as occupied, provided that the site is located within a region for which the occurrence of the respective species is actually documented[33]. We assumed that the populations at these sites initially had adult numbers according to their respective carrying capacities. We started simulations in the year 1990 to allow the hybrid models a burn-in phase from these initial settings. To account for stochastic elements in the models, runs for each species were repeated 10 times for both the low and the high demographic and dispersal parameter sets. However, with respect to the reported statistics (range size, i.e. number of cells occupied), the variability among runs within one

particular parameter set was negligibly small. We hence only report the average values of these 10 runs, respectively.

Analysis

For each year, we computed the number of sites predicted to be occupied by a species. Projections of the niche-based models were translated to binary occupancy using, again, prevalence as the threshold. For no-dispersal niche model predictions, occupancy at any year was additionally constrained to those sites that had been occupied in the previous year. The proportions of suitable but unoccupied, and occupied but unsuitable sites, respectively, were derived from a simple overlay between niche-based and hybrid model projections.

Sensitivity analysis

We quantified the sensitivity of simulation outcomes to uncertainty in the various demographic and dispersal parameter estimates by means of a Monte Carlo approach. Essentially, this analysis is based on running simulations with parameter values randomly drawn from specified distributions. Here, we defined these distributions as uniform and bounded between the low and high values given in Supplementary Table 1. In case of the minimum age of maturity, the discrete values of 1, 2 and 5 years were varied in the range of 0, 1 and 2 years, respectively, i.e. age of maturity was kept constant for annual plants, while for species maturing in the second or fifth year values were randomly drawn from the intervals [1, 3] and [3, 7], respectively. For the proportions of exo- and endozoochorous dispersal we assumed uniform distributions between 0% and 5%.

In total, we executed 585 simulations with combinations of such randomly drawn parameter values for each of 10 randomly selected species. We analysed the results by means of the variance decomposition procedure described in Saltelli *et al.*[34] and implemented in

SIMLAB[35], a development framework for sensitivity and uncertainty analysis. The procedure delivers, for each parameter, a (model-free) sensitivity measure that represents the expected residual variance in model outcomes if all but the respective parameter values could be fixed[34]. The measure includes all effects of any order that include the respective parameter ('total order effect'[34])and is scaled between 0 (no influence on results) and 1 (all variation in model outcomes due to this single parameter).

The ten species were selected such that we first grouped all species by the amount of range change predicted by the hybrid models (as represented in Supplementary Fig. S1) and then randomly draw representatives from these groups.

Quantification of extinction debt

To provide a quantitative estimate of the lag times in local population extinction we recorded for each 100 m × 100 m cell occupied by a particular species in each simulation run the year when niche models predicted this cell to become unsuitable for the respective species and the year when hybrid models predicted the local population to have become extinct. For reasons of memory space, this information was only stored at a 10-year resolution. In case that becoming unsuitable and extinction happened within the same decade for a cell and its population, we assumed a lag of 1 year between the two events as a conservative assumption with respect to extinction debt length. As simulations were only run until the year 2100, and not until all populations in unsuitable cells had finally become extinct, we interpreted these data as right-censored time-to-event data and calculated, for each species, empirical survival functions based on the Kaplan-Meier algorithm[36]. To get an estimate of lag times longer than the simulation interval we also fitted parametric survival models to the same data assuming that lag times follow Weibull distributions. The fitted models were then used to predict the mean delay of population extinction across all cells occupied by a species and becoming climatically unsuitable during the simulation run.

Survival models were fitted by means of the *survreg* function in the R-package *survival*[37]. Simulations from hybrid models with high and low demographic and dispersal parameter values were pooled for this analysis because local population dynamics converge when cells become unsuitable: such cells are sinks with no own seed yield (see chapter "Demographic models") and hence persistence time mainly depends on clonal propagation which falls below 1 in unsuitable cells irrespective of the maximum values assumed under well suited conditions.

Supplementary figures

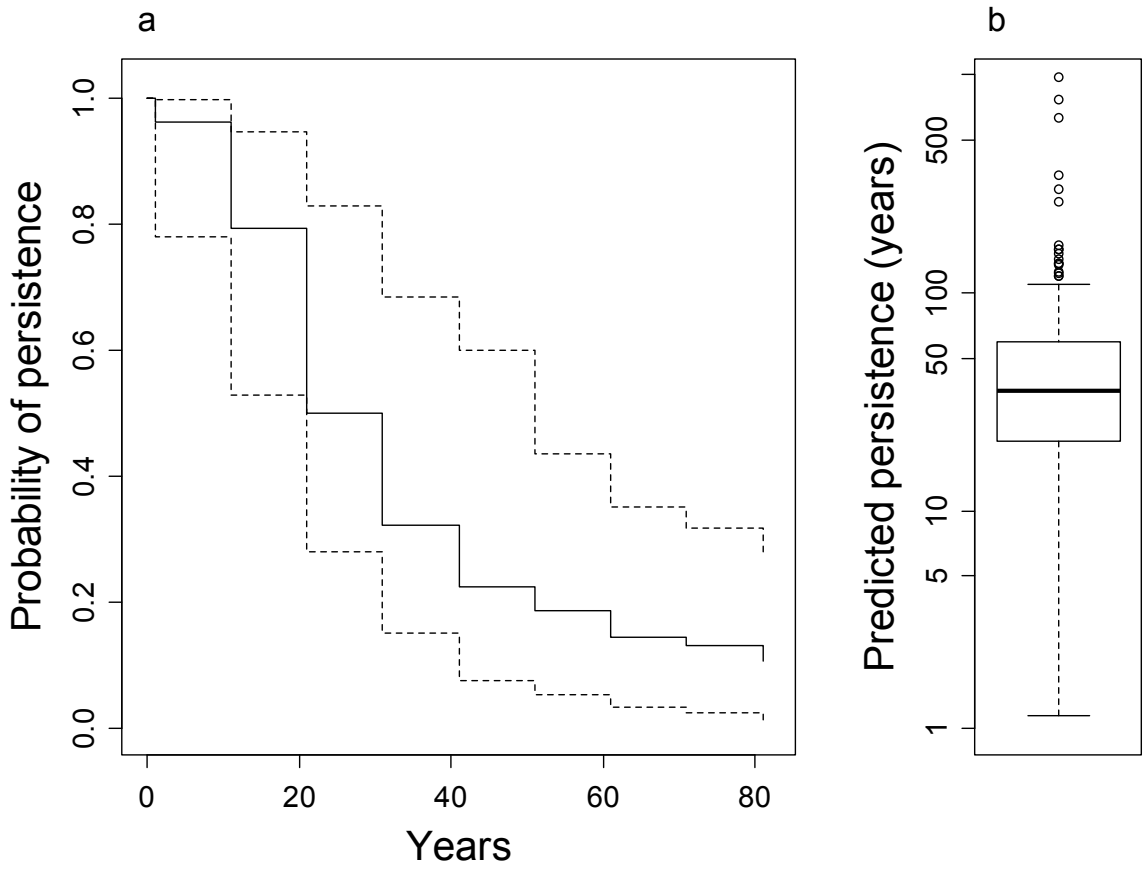

Fig. S1 Simulated lag times of population extinctions. a: Kaplan-Meier survival function providing the empirical probability that a cell predicted to have become climatically unsuitable to a species by the niche model is still predicted to harbour a local population of this species after *x* years by the hybrid model. The solid line is the median and the dashed lines are the 0.25 and 0.75 quantiles of these probabilities across all species. b: the distribution of species-specific estimates of these lag times derived from parametric survival models fitted to the same data. The bold line represents the median predicted extinction lag across all species and cells. Note that the y-axis is log-scaled. For details of calculation see Supplementary Methods.

Fig. S2 Proportion of species predicted to have lost or gained a certain percentage of their current range size by the end of the 21st century. Red bars represent results from hybrid models with demographic and dispersal parameters set to high (b,b') and low (c,c') values, respectively. Bars b and c refer to loss calculations based on the number of sites predicted to be occupied, bars b' and c' to loss calculations based on the number of sites predicted to be both occupied and still climatically suitable to the species. Grey bars represent results of niche-based projections under unlimited (a) or no (f) dispersal assumptions.

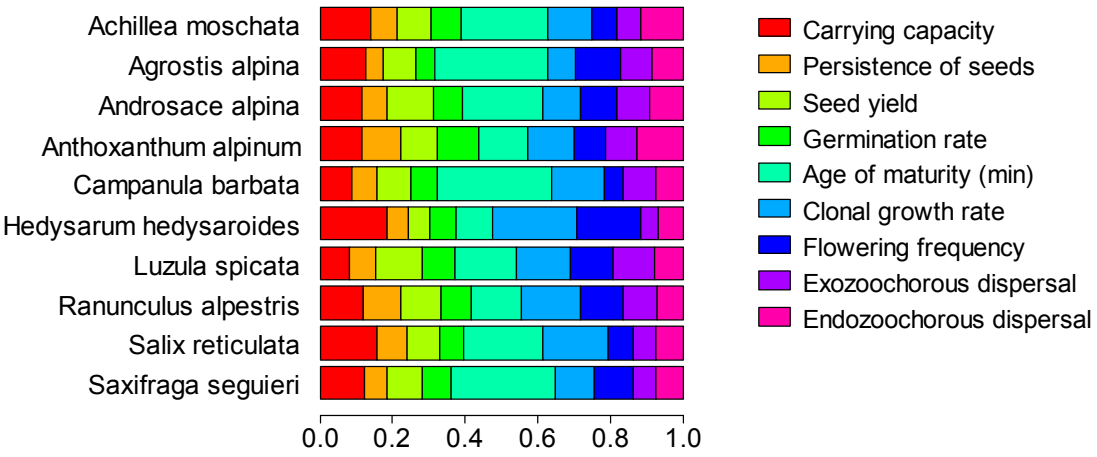

Fig. S3 Sensitivity of hybrid model simulations to variation in demographic and dispersal parameters. Calculations were done for 10 species randomly selected from species groups defined by the amount of predicted range size change (see Supplementary Fig. S1). Color bars represent the expected residual variance in simulation results if all but the respective parameter could be fixed to known values. Values were transformed to sum up to 1 to facilitate comparisons among species. High values identify uncertainties in the estimation of the concerned parameter to be highly influential on predicted changes in range size. For details of calculation see Supplementary Methods.

Supplementary tables

Supplementary Table 1: List of species selected for modelling, their maximum demographic rates under well-suited environmental conditions, and their traits relevant for establishing dispersal kernels.

Species name	Mat	Age	SP_l	SP_h	CC	CIG_l	CIG_h	FF_l	FF_h	JS_l	JS_h	SY_l	SY_h	Germ_l	Germ_h	vt	H0	h	GS	DR
Achillea atrata	2 - 5	100	5	5	296250	**2.00**	**5.00**	0.15	0.30	0.41	0.58	10	100	**0.03**	**0.10**	0.92	0.2	0,01	0.035	53.1
Achillea clavennae	2 - 5	100	5	5	985500	**0.25**	**0.75**	0.15	0.30	0.41	0.58	10	100	0.03	0.10	2.00	0.25	0,1	0.025	47.1
Achillea clusiana	2 - 5	100	5	5	950000	2.00	5.00	0.20	0.40	0.41	0.58	10	100	**0.06**	**0.18**	1.40	0.2	0,01	0.026	47.8
Achillea moschata	2 - 5	100	**5**	**5**	462750	2.00	5.00	0.15	0.30	0.41	0.58	10	100	**0.05**	**0.10**	1.85	0.2	0,01	0.048	58.9
Adenostyles alliariae	2 - 5	100	**1**	**1**	75000	**0.25**	**0.75**	0.15	0.35	0.41	0.58	100	1000	0.11	0.22	0.85	1.2	0,7	0.017	51.5
Agrostis alpina	2 - 5	100	**1**	**1**	157500000	**2.00**	**5.00**	0.20	0.40	0.41	0.58	10	100	0.04	0.08	1.57	0.3	0,1	0.071	65.3
Agrostis rupestris	2 - 5	100	**5**	**5**	67500000	**2.00**	**5.00**	0.20	0.40	0.41	0.58	10	100	0.04	0.08	1.47	0.1	0,1	0.071	65.3
Agrostis schraderiana	2 - 5	100	1	5	14500000	**2.00**	**5.00**	0.20	0.40	0.41	0.58	10	100	0.04	0.08	0.39	0.6	0,1	0.089	65.4
Alchemilla anisiaca	2 - 5	100	1	1	518750	1.00	5.00	0.15	0.30	0.41	0.58	10	100	0.11	0.22	1.68	0.2	0,1	0.027	48.5
Androsace alpina	2 - 5	100	**1**	**1**	3225000	1.00	5.00	0.20	0.40	0.41	0.58	10	100	0.11	0.22	2.16	0.05	0,01	0.032	51.4
Androsace obtusifolia	2 - 5	100	**1**	**1**	480000	**0.25**	**0.75**	0.20	0.35	0.41	0.58	10	100	0.11	0.22	2.67	0.1	0,1	0.023	44.9
Anemone narcissiflora	2 - 5	100	1	1	33550	**1.00**	**1.00**	0.20	0.35	0.41	0.58	10	100	0.11	0.22	1.92	0.5	0,1	0.005	5.7
Antennaria carpatica	2 - 5	100	**1**	**1**	778500	**1.00**	**1.00**	0.10	0.20	0.41	0.58	10	100	0.11	0.22	0.21	0.15	0,1	0.049	63.7
Antennaria dioica	**2 - 5**	100	**1**	**1**	2193750	**2.00**	**5.00**	0.10	0.20	0.41	0.58	10	100	0.11	0.22	0.17	0.2	0,1	0.086	65.5
Anthoxanthum alpinum	2 - 5	100	**10**	**10**	22500000	**1.00**	**1.00**	0.15	0.30	0.41	0.58	10	100	0.04	0.08	1.65	0.255	0,1	0.027	58.5
Anthyllis vulneraria sssp.alpestris	**2 - 5**	100	**10**	**10**	438750	0.25	0.75	0.20	0.40	0.41	0.58	10	100	**0.06**	**0.12**	2.00	0.2	0,1	0.002	10.3
Arabis alpina	2 - 5	100	**5**	**10**	119250	**0.25**	**0.75**	0.20	0.40	0.41	0.58	10	100	0.11	0.22	1.50	0.4	0,01	0.044	31.8
Arabis caerulea	2 - 5	100	**10**	**10**	378000	**0.25**	**0.75**	0.10	0.25	0.41	0.58	10	100	**0.02**	**0.10**	1.42	0.12	0,01	0.040	30.4
Arenaria biflora	2 - 5	100	**10**	**10**	660000	0.25	0.75	0.20	0.35	0.41	0.58	10	100	0.11	0.22	2.16	0.03	0,01	0.060	62.8
Arenaria ciliata	2 - 5	100	10	10	1080000	**0.25**	**0.75**	0.20	0.35	0.41	0.58	10	100	0.11	0.22	3.07	0.07	0,1	0.057	62.0
Armeria alpina	2 - 5	100	5	10	1350000	0.25	1.00	0.10	0.20	0.41	0.58	10	100	0.11	0.22	2.24	0.25	0,1	0.007	9.7
Aster bellidiastrum	2 - 5	100	1	1	412500	**0.25**	**0.75**	0.20	0.40	0.41	0.58	10	100	0.11	0.22	0.25	0.25	0,1	0.044	62.8
Avenula versicolor	2 - 5	100	**1**	**1**	12480000	2.00	5.00	0.20	0.35	0.41	0.58	10	100	0.04	0.08	1.99	0.4	0,1	0.013	53.0
Bartsia alpina	2 - 5	100	**1**	**1**	2415000	**0.25**	**0.75**	0.25	0.50	0.41	0.58	**100**	**1000**	0.11	0.22	1.82	0.15	0,1	0.030	50.4
Biscutella laevigata ssp. laevigata	2 - 5	100	**5**	**10**	2047500	**0.25**	**0.75**	0.20	0.35	0.41	0.58	100	1000	0.11	0.22	1.58	0.4	0,1	0.007	8.5
Campanula alpina	2 - 5	100	1	10	765000	0.25	0.75	0.15	0.25	0.41	0.58	100	1000	0.11	0.22	1.65	0.2	0,1	0.028	25.2
Campanula barbata	2 - 5	100	**1**	**1**	652500	**0.25**	**0.75**	0.15	0.25	0.41	0.58	100	1000	0.11	0.22	1.42	0.4	0,1	0.166	75.1
Campanula pulla	2 - 5	100	1	10	1560000	0.25	0.75	**0.15**	**0.15**	0.41	0.58	100	1000	0.11	0.22	1.22	0.15	0,01	0.153	74.6
Campanula scheuchzeri	2 - 5	100	**5**	**10**	3300000	**0.25**	**0.75**	0.15	0.30	0.41	0.58	100	1000	0.11	0.22	1.42	0.3	0,1	0.065	64.1

Species name	Mat	Age	SP_l	SP_h	CC	CIG_l	CIG_h	FF_l	FF_h	JS_l	JS_h	SY_l	SY_h	Germ_l	Germ_h	vt	H0	h	GS	DR
Carex atrata	2 - 5	100	1	10	4500000	**1.00**	**1.00**	0.15	0.25	0.41	0.58	100	1000	0.04	0.08	2.43	0.27	0,1	0.023	45.0
Carex capillaris	2 - 5	100	**1**	**1**	20587500	**2.00**	**5.00**	0.15	0.30	0.41	0.58	10	100	0.04	0.08	2.84	0.3	0,1	0.023	45.0
Carex firma	2 - 5	100	**5**	**10**	13125000	**0.25**	**0.75**	0.20	0.40	0.41	0.58	10	100	0.04	0.08	2.36	0.2	0,1	0.016	50.7
Carex frigida	2 - 5	100	**1**	**1**	3712500	**2.00**	**5.00**	0.15	0.30	0.41	0.58	10	100	0.04	0.08	1.19	0.4	0,1	0.034	60.5
Carex sempervirens	2 - 5	100	**5**	**10**	42500000	**2.00**	**5.00**	0.15	0.30	0.41	0.58	10	100	0.04	0.08	2.96	0.4	0,1	0.015	50.0
Cerastium cerastoides	2 - 5	100	**10**	**10**	1192500	**2.00**	**5.00**	0.20	0.40	0.41	0.58	10	100	0.11	0.22	2.01	0.03	0,01	0.052	60.4
Cerastium pedunculatum	2 - 5	100	**10**	**10**	900000	2.00	5.00	0.25	0.50	0.41	0.58	10	100	0.11	0.22	1.42	0.1	0,01	0.064	63.9
Cerastium uniflorum	2 - 5	100	**1**	**1**	2887500	**0.25**	**0.75**	0.25	0.50	0.41	0.58	10	100	0.11	0.22	1.70	0.08	0,01	0.039	55.2
Crepis aurea	2 - 5	100	**1**	**1**	777500	**1.00**	**1.00**	0.20	0.35	0.41	0.58	10	100	0.11	0.22	1.07	0.2	0,1	0.025	56.8
Dianthus alpinus	2 - 5	100	5	10	432000	0.25	5.00	0.15	0.30	0.41	0.58	10	100	0.11	0.22	2.35	0.1	0,1	0.022	21.8
Doronicum clusii	2 - 5	100	**1**	**1**	11475	0.25	0.75	0.20	0.35	0.41	0.58	100	1000	0.11	0.22	0.94	0.4	0,1	0.020	53.5
Draba dubia	2 - 5	100	**10**	**10**	260000	**0.25**	**0.75**	0.20	0.35	0.41	0.58	10	100	0.11	0.22	1.41	0.14	0,01	0.084	68.1
Draba stellata	2 - 5	100	10	10	100000	0.25	0.75	0.20	0.35	0.41	0.58	10	100	0.11	0.22	2.03	0.1	0,01	0.043	57.1
Dryas octopetala	**2 - 5**	100	**1**	**1**	40200000	**0.25**	**0.75**	0.25	0.50	0.41	0.58	**10**	**100**	**0.20**	**0.20**	0.55	0.15	0,1	0.022	55.4
Epilobium anagallidifolium	**1 - 1**	**1**	**5**	**5**	135000	**0.00**	**0.00**	0.25	0.45	0.17	0.33	**100**	**1000**	0.11	0.22	0.20	0.07	0,01	0.089	65.4
Erigeron uniflorus	2 - 5	100	**5**	**10**	226800	**1.00**	**1.00**	0.20	0.40	0.41	0.58	10	100	0.11	0.22	1.30	0.1	0,1	0.044	62.8
Festuca halleri s.str.	2 - 5	100	**5**	**10**	40468750	2.00	5.00	0.15	0.30	0.41	0.58	10	100	0.04	0.08	1.38	0.25	0,1	0.043	62.6
Festuca nigricans	2 - 5	100	**1**	**1**	21225000	**2.00**	**5.00**	0.15	0.30	0.41	0.58	10	100	0.04	0.08	1.97	0.5	0,1	0.014	48.0
Festuca pseudodura	2 - 5	100	1	10	59625000	2.00	5.00	0.15	0.30	0.41	0.58	100	1000	0.04	0.08	1.81	0.4	0,1	0.026	57.5
Festuca pumila	2 - 5	100	**5**	**10**	53812500	**2.00**	**5.00**	0.15	0.30	0.41	0.58	10	100	0.04	0.08	2.24	0.2	0,1	0.025	56.7
Festuca rupicaprina	2 - 5	100	1	10	26512500	2.00	5.00	0.15	0.30	0.41	0.58	10	100	0.04	0.08	1.08	0.2	0,1	0.025	56.8
Galium anisophyllon	2 - 5	100	**5**	**5**	7680000	**0.25**	**0.75**	0.25	0.50	0.41	0.58	10	100	0.11	0.22	2.74	0.2	0,1	0.026	47.5
Gentiana acaulis	2 - 5	100	**1**	**1**	414000	**0.25**	**0.75**	0.20	0.40	0.41	0.58	10	100	0.11	0.22	2.75	0.1	0,1	0.034	52.8
Gentiana bavarica	2 - 5	100	**1**	**1**	4500000	**0.25**	**0.75**	0.15	0.25	0.41	0.58	10	100	0.11	0.22	1.49	0.15	0,01	0.101	70.4
Gentiana clusii	2 - 5	100	**5**	**10**	118800	**0.25**	**0.75**	0.20	0.40	0.41	0.58	10	100	0.11	0.22	2.76	0.1	0,1	0.027	48.2
Gentiana nivalis	**1 - 1**	**1**	**1**	**1**	840000	**0.00**	**0.00**	0.50	1.00	0.17	0.33	**100**	**1000**	0.11	0.22	1.14	0.15	0,1	0.161	74.9
Gentiana pumila	2 - 5	100	**10**	**10**	240000	0.25	0.75	0.20	0.40	0.41	0.58	10	100	0.11	0.22	1.40	0.12	0,1	0.099	70.2
Gentiana punctata	2 - 5	100	**1**	**1**	51750	**0.25**	**0.75**	0.15	0.30	0.41	0.58	100	1000	0.11	0.22	1.93	0.6	0,1	0.020	20.5
Gentiana verna ssp. verna	**2 - 5**	100	**5**	**10**	540000	**0.25**	**0.75**	0.20	0.40	0.41	0.58	10	100	0.11	0.22	1.26	0.1	0,1	0.079	67.1
Gentianella campestris	**1 - 1**	**1**	1	10	144000	0.00	0.00	0.30	0.60	0.41	0.58	**10**	**100**	0.11	0.22	2.74	0.2	0,1	0.042	56.7
Geum montanum	2 - 5	100	**1**	**1**	320000	**0.25**	**0.75**	0.20	0.35	0.41	0.58	10	100	0.11	0.22	1.43	0.4	0,1	0.013	47.4
Geum reptans	2 - 5	100	**1**	**1**	62000	**0.25**	**0.75**	0.20	0.35	0.41	0.58	10	100	**0.005**	**0.01**	0.83	0.15	0,01	0.018	52.4
Gnaphalium hoppeanum	2 - 5	100	**1**	**1**	672000	**0.25**	**0.75**	0.20	0.35	0.41	0.58	10	100	**0.08**	**0.28**	0.45	0.1	0,01	0.072	65.4
Gnaphalium supinum	2 - 5	100	**5**	**5**	2248750	**1.00**	**1.00**	0.20	0.35	0.41	0.58	10	100	0.08	0.28	0.48	0.1	0,01	0.091	65.4
Hedysarum hedysaroides ssp. hedysaroides	2 - 5	100	1	1	247500	0.25	0.75	0.20	0.40	0.41	0.58	10	100	0.10	0.18	2.32	0.3	0,1	0.005	6.5
Helianthemum alpestre	5 - 10	100	**5**	**10**	4200000	**0.25**	**0.75**	0.30	0.55	0.70	0.80	10	100	0.10	0.25	3.28	0.15	0,1	0.022	44.5
Helianthemum grandiflorum	**5 - 10**	100	**5**	**10**	4068750	0.25	0.75	0.30	0.55	0.70	0.80	10	100	0.10	0.25	3.51	0.2	0,1	0.012	32.7
Hieracium alpinum	2 - 5	100	**1**	**1**	275625	**1.00**	**1.00**	0.20	0.45	0.41	0.58	10	100	0.11	0.22	1.32	0.3	0,1	0.016	50.7

Species name	Mat	Age	SP_l	SP_h	CC	CIG_l	CIG_h	FF_l	FF_h	JS_l	JS_h	SY_l	SY_h	Germ_l	Germ_h	vt	H0	h	GS	DR
Hieracium intybaceum	2 - 5	100	**1**	**1**	53250	**1.00**	**1.00**	0.20	0.45	0.41	0.58	10	100	0.11	0.22	0.97	0.3	0,01	0.021	54.2
Homogyne alpina	2 - 5	100	**1**	**1**	3187500	**0.25**	**0.75**	0.10	0.20	0.41	0.58	10	100	0.11	0.22	0.42	0.3	0,1	0.017	51.3
Hypochoeris uniflora	2 - 5	100	1	1	205500	0.25	1.00	0.25	0.55	0.41	0.58	10	100	0.11	0.22	1.41	0.5	0,1	0.006	35.6
Juncus jacquinii	2 - 5	100	**1**	**1**	23250000	**2.00**	**5.00**	0.15	0.30	0.41	0.58	10	100	0.04	0.08	0.98	0.25	0,1	0.170	75.3
Juncus monanthos	2 - 5	100	1	1	13725000	2.00	5.00	0.15	0.30	0.41	0.58	10	100	0.04	0.08	1.53	0.25	0,1	0.049	59.3
Juncus trifidus	2 - 5	100	**1**	**1**	38250000	**2.00**	**5.00**	0.15	0.30	0.41	0.58	10	100	0.04	0.08	1.59	0.24	0,1	0.057	62.1
Kobresia myosuroides	2 - 5	100	**1**	**1**	39750000	**2.00**	**5.00**	0.15	0.30	0.41	0.58	10	100	0.04	0.08	2.67	0.3	0,1	0.023	45.3
Leontodon helveticus	2 - 5	100	**5**	**5**	581250	**2.00**	**5.00**	0.20	0.35	0.41	0.58	10	100	0.11	0.22	1.35	0.2	0,1	0.014	48.8
Leontopodium alpinum	2 - 5	100	**5**	**5**	823500	**0.25**	**0.75**	0.15	0.30	0.41	0.58	10	100	0.11	0.22	0.28	0.2	0,1	0.052	64.1
Leucanthemopsis alpina	2 - 5	100	**5**	**5**	2110000	**1.00**	**1.00**	0.20	0.25	0.41	0.58	10	100	0.11	0.22	1.78	0.15	0,1	0.032	51.8
Ligusticum mutellina	2 - 5	100	**5**	**10**	1155000	**0.25**	**0.75**	0.15	0.30	0.41	0.58	10	100	0.11	0.22	3.18	0.5	0,1	0.007	24.1
Ligusticum mutellinoides	2 - 5	100	1	1	264600	**0.25**	**0.75**	0.15	0.30	0.41	0.58	10	100	0.11	0.22	2.04	0.15	0,1	0.015	37.0
Lloydia serotina	2 - 5	100	**10**	**10**	375000	**2.00**	**5.00**	0.20	0.35	0.41	0.58	**10**	**100**	0.11	0.22	1.58	0.1	0,1	0.035	53.1
Loiseleuria procumbens	**2 - 5**	100	**1**	**1**	21000000	**0.25**	**0.75**	0.20	0.35	0.41	0.58	10	100	0.10	0.25	1.15	0.035	0,1	0.220	76.3
Luzula alpinopilosa	2 - 5	100	**1**	**1**	13250000	0.25	5.00	0.15	0.30	0.41	0.58	100	1000	0.04	0.08	2.52	0.3	0,01	0.043	57.0
Luzula glabrata	2 - 5	100	1	10	5092500	**0.25**	**0.75**	0.15	0.30	0.41	0.58	100	1000	0.04	0.08	3.16	0.3	0,1	0.025	46.9
Luzula lutea	2 - 5	100	**10**	**10**	5512500	0.25	0.75	0.15	0.30	0.41	0.58	10	100	0.04	0.08	2.90	0.2	0,1	0.076	66.6
Luzula spicata	2 - 5	100	**5**	**10**	4492500	**2.00**	**5.00**	0.15	0.30	0.41	0.58	10	100	0.04	0.08	2.60	0.25	0,1	0.033	52.3
Minuartia gerardii	2 - 5	100	**5**	**5**	6900000	0.25	0.75	0.20	0.35	0.41	0.58	10	100	0.11	0.22	1.92	0.1	0,1	0.060	62.9
Minuartia sedoides	5 - 10	100	**1**	**1**	25968750	**0.25**	**0.75**	0.15	0.30	0.70	0.80	10	100	0.11	0.22	2.73	0.08	0,1	0.037	54.5
Moehringia ciliata	2 - 5	100	5	5	1975000	**0.25**	**0.75**	0.20	0.40	0.41	0.58	10	100	0.11	0.22	3.00	0.2	0,01	0.029	49.6
Myosotis alpestris	**2 - 5**	100	**5**	**10**	345000	**1.00**	**1.00**	0.20	0.45	0.41	0.58	**10**	**100**	0.11	0.22	2.03	0.2	0,1	0.026	47.7
Oreochloa disticha	2 - 5	100	**5**	**10**	34687500	**2.00**	**5.00**	0.15	0.30	0.41	0.58	10	100	0.04	0.08	1.88	0.2	0,1	0.032	51.6
Oxyria digyna	**2 - 5**	100	**1**	**1**	798000	**0.25**	**0.75**	0.25	0.45	0.41	0.58	10	100	**0.05**	**0.10**	0.83	0.15	0,01	0.021	21.7
Oxytropis campestris ssp. campestris	2 - 5	100	1	1	320250	0.25	0.75	0.20	0.40	0.41	0.58	10	100	0.10	0.18	2.74	0.2	0,1	0.011	31.6
Pedicularis aspleniifolia	2 - 5	100	**5**	**5**	49500	2.00	5.00	0.20	0.40	0.41	0.58	10	100	0.11	0.22	3.01	0.08	0,01	0.029	49.7
Pedicularis oederi	2 - 5	100	1	10	144000	**2.00**	**5.00**	0.20	0.40	0.41	0.58	10	100	0.11	0.22	3.51	0.095	0,1	0.015	37.0
Pedicularis portenschlagii	2 - 5	100	1	10	52500	2.00	5.00	0.20	0.40	0.41	0.58	10	100	0.11	0.22	3.39	0.08	0,1	0.015	36.6
Pedicularis rostratocapitata	2 - 5	100	**1**	**1**	360000	2.00	5.00	0.20	0.40	0.41	0.58	10	100	0.11	0.22	3.26	0.2	0,1	0.013	34.0
Pedicularis verticillata	2 - 5	100	**10**	**10**	234000	2.00	5.00	0.20	0.40	0.41	0.58	10	100	0.11	0.22	2.19	0.3	0,1	0.018	40.6
Persicaria vivipara	2 - 5	100	**5**	**5**	6750000	0.25	5.00	0.40	0.80	0.41	0.58	10	100	0.11	0.22	3.64	0.3	0,1	0.008	26.3
Peucedanum ostruthium	2 - 5	100	**1**	**1**	97500	**0.25**	**0.75**	0.25	0.45	0.41	0.58	100	1000	0.11	0.22	1.61	1	0,1	0.012	14.9
Phleum commutatum	2 - 5	100	**1**	**1**	4965000	**0.25**	**0.75**	0.15	0.30	0.41	0.58	10	100	0.04	0.08	0.90	0.4	0,1	0.027	57.8
Phyteuma hemisphaericum	2 - 5	100	**1**	**1**	429750	**0.25**	**0.75**	0.20	0.40	0.41	0.58	10	100	0.11	0.22	1.62	0.15	0,1	0.081	67.4
Poa alpina	2 - 5	100	**5**	**5**	68750000	**0.00**	**1.00**	0.15	0.30	0.41	0.58	**10**	**100**	0.04	0.08	1.27	0.26	0,1	0.033	52.0
Poa laxa	**2 - 5**	100	**1**	**1**	6000000	2.00	5.00	0.20	0.35	0.41	0.58	10	100	0.04	0.08	1.38	0.2	0,01	0.036	53.9
Poa minor	2 - 5	100	1	1	6680000	**2.00**	**5.00**	0.20	0.35	0.41	0.58	10	100	0.04	0.08	1.59	0.25	0,01	0.030	50.4
Potentilla aurea	2 - 5	100	**1**	**1**	1980000	**0.25**	**0.75**	0.25	0.45	0.41	0.58	10	100	0.11	0.22	2.05	0.2	0,1	0.039	55.4

Species name	Mat	Age	SP_l	SP_h	CC	CIG_l	CIG_h	FF_l	FF_h	JS_l	JS_h	SY_l	SY_h	Germ_l	Germ_h	vt	H0	h	GS	DR
Potentilla brauneana	2 - 5	100	**1**	**1**	221625	**0.25**	**0.75**	0.25	0.45	0.41	0.58	10	100	0.11	0.22	2.98	0.5	0,01	0.025	46.8
Potentilla clusiana	2 - 5	100	1	1	618750	**0.25**	**0.75**	0.25	0.50	0.41	0.58	10	100	0.11	0.22	0.94	0.1	0,01	0.042	62.5
Primula clusiana	2 - 5	100	10	10	783000	**1.00**	**1.00**	0.20	0.35	0.41	0.58	100	1000	0.11	0.22	2.23	0.1	0,1	0.033	52.1
Primula glutinosa	2 - 5	100	**10**	**10**	1085625	1.00	1.00	0.20	0.45	0.41	0.58	10	100	0.11	0.22	1.97	0.08	0,1	0.056	61.8
Primula hirsuta	2 - 5	100	**10**	**10**	115200	**1.00**	**1.00**	0.20	0.40	0.41	0.58	100	1000	0.11	0.22	2.14	0.07	0,01	0.058	62.4
Primula minima	2 - 5	100	**5**	**5**	3100000	**1.00**	**1.00**	0.20	0.35	0.41	0.58	10	100	0.11	0.22	1.88	0.04	0,1	0.062	63.5
Pritzelago alpina	2 - 5	100	**5**	**10**	3165000	0.25	0.75	0.20	0.40	0.41	0.58	10	100	0.11	0.22	2.63	0.1	0,01	0.026	47.5
Ranunculus alpestris	2 - 5	100	**1**	**1**	1920000	**1.00**	**1.00**	0.20	0.45	0.41	0.58	10	100	0.11	0.22	2.06	0.15	0,1	0.039	55.2
Ranunculus glacialis	2 - 5	100	**1**	**1**	967500	**1.00**	**1.00**	0.20	0.40	0.41	0.58	**10**	**100**	0.11	0.22	1.71	0.15	0,01	0.026	24.0
Rhododendron ferrugineum	5 - 10	100	**1**	**1**	43125	0.25	0.75	0.20	0.45	0.70	0.80	100	1000	0.10	0.25	0.89	1.5	0,1	0.202	76.0
Salix herbacea	5 - 10	100	**1**	**1**	7500000	**0.25**	**0.75**	0.25	0.45	0.70	0.80	100	1000	0.10	0.25	0.24	0.022	0,01	0.047	63.3
Salix reticulata	5 - 10	100	**1**	**1**	1650000	**1.00**	**1.00**	0.20	0.40	0.70	0.80	100	1000	0.10	0.25	0.25	0.04	0,01	0.056	64.5
Salix retusa	5 - 10	100	**5**	**10**	12200000	1.00	1.00	0.20	0.35	0.70	0.80	100	1000	0.10	0.25	0.26	0.3	0,01	0.026	57.5
Saponaria pumila	2 - 5	100	5	5	2756250	0.25	5.00	0.15	0.30	0.41	0.58	10	100	0.11	0.22	3.47	0.05	0,1	0.013	34.2
Saussurea pygmaea	2 - 5	100	1	1	360000	0.25	1.00	0.20	0.35	0.41	0.58	10	100	0.11	0.22	0.71	0.2	0,1	0.005	32.1
Saxifraga aizoides	2 - 5	100	**10**	**10**	6937500	**0.25**	**0.75**	0.15	0.30	0.41	0.58	100	1000	**0.05**	**0.10**	1.23	0.3	0,01	0.111	71.5
Saxifraga androsacea	2 - 5	100	**10**	**10**	2750000	**2.00**	**5.00**	0.20	0.40	0.41	0.58	100	1000	0.05	0.10	1.46	0.1	0,01	0.135	73.6
Saxifraga bryoides	2 - 5	100	**5**	**5**	8250000	**0.25**	**0.75**	0.20	0.35	0.41	0.58	100	1000	0.05	0.10	0.89	0.08	0,01	0.158	74.8
Saxifraga caesia	2 - 5	100	**1**	**1**	7950000	**0.25**	**0.75**	0.20	0.35	0.41	0.58	100	1000	0.05	0.10	1.35	0.1	0,1	0.155	74.7
Saxifraga exarata	2 - 5	100	1	10	2520000	0.25	0.75	0.20	0.35	0.41	0.58	100	1000	0.05	0.10	1.15	0.1	0,1	0.165	75.1
Saxifraga moschata	2 - 5	100	**1**	**1**	4125000	**0.25**	**0.75**	0.20	0.35	0.41	0.58	100	1000	0.05	0.10	1.59	0.1	0,1	0.117	72.2
Saxifraga oppositifolia	**2 - 5**	100	**10**	**10**	10312500	**0.25**	**0.75**	0.15	0.30	0.41	0.58	**100**	**1000**	**0.05**	**0.10**	1.26	0.06	0,01	0.066	64.5
Saxifraga paniculata	2 - 5	100	**1**	**1**	3325000	**0.25**	**0.75**	0.15	0.30	0.41	0.58	100	1000	0.05	0.10	1.62	0.3	0,01	0.104	70.9
Saxifraga seguieri	2 - 5	100	**10**	**10**	2411500	0.25	0.75	0.20	0.35	0.41	0.58	100	1000	0.05	0.10	1.67	0.08	0,01	0.111	71.6
Saxifraga stellaris	2 - 5	100	**10**	**10**	918750	**2.00**	**5.00**	0.25	0.50	0.41	0.58	**100**	**1000**	0.05	0.10	1.36	0.1	0,01	0.124	72.7
Sedum atratum	**1 - 1**	**1**	**5**	**10**	384000	0.00	0.00	0.25	0.45	0.41	0.58	100	1000	0.11	0.22	1.18	0.08	0,01	0.155	74.7
Sempervivum montanum	2 - 5	100	5	10	471000	1.00	5.00	0.15	0.30	0.41	0.58	100	1000	0.11	0.22	1.19	0.12	0,01	0.233	76.4
Senecio doronicum ssp. doronicum	2 - 5	100	1	1	147187.5	**2.00**	**5.00**	0.20	0.35	0.41	0.58	10	100	0.11	0.22	0.52	0.5	0,1	0.018	52.1
Sibbaldia procumbens	**2 - 5**	100	**1**	**1**	727500	**0.25**	**0.75**	0.20	0.35	0.41	0.58	10	100	0.11	0.22	3.04	0.05	0,01	0.026	47.4
Silene acaulis ssp. exscapa	5 - 10	100	**5**	**10**	20100000	2.00	5.00	0.20	0.35	0.70	0.80	100	1000	0.11	0.22	2.90	0.03	0,1	0.023	45.0
Silene acaulis ssp. longiscapa	5 - 10	100	**5**	**10**	25500000	**2.00**	**5.00**	0.20	0.35	0.70	0.80	100	1000	0.11	0.22	3.08	0.03	0,1	0.020	42.3
Silene rupestris	2 - 5	100	5	10	502500	**0.25**	**0.75**	0.20	0.40	0.41	0.58	100	1000	0.11	0.22	2.05	0.2	0,01	0.082	67.7
Soldanella alpina	2 - 5	100	**1**	**1**	806250	**1.00**	**1.00**	0.10	0.20	0.41	0.58	10	100	0.11	0.22	2.67	0.2	0,1	0.039	55.3
Soldanella pusilla	2 - 5	100	**5**	**10**	2992500	1.00	1.00	0.10	0.20	0.41	0.58	10	100	0.11	0.22	2.31	0.1	0,01	0.075	66.3
Thalictrum alpinum	**2 - 5**	100	**5**	**5**	360000	2.00	5.00	0.10	0.25	0.41	0.58	10	100	0.11	0.22	2.70	0.15	0,1	0.020	42.3
Thesium alpinum	2 - 5	100	**1**	**1**	817500	**0.25**	**0.75**	0.30	0.60	0.41	0.58	10	100	0.11	0.22	2.58	0.25	0,1	0.011	45.0
Trifolium badium	2 - 5	100	**1**	**1**	877500	**0.25**	**0.75**	0.25	0.50	0.41	0.58	10	100	0.10	0.22	0.98	0.2	0,1	0.016	17.9
Trifolium pallescens	2 - 5	100	**10**	**10**	2231250	0.25	0.75	0.20	0.45	0.41	0.58	10	100	**0.06**	**0.12**	3.07	0.2	0,01	0.018	19.7

Species name	Mat	Age	SP_l	SP_h	CC	CIG_l	CIG_h	FF_l	FF_h	JS_l	JS_h	SY_l	SY_h	Germ_l	Germ_h	vt	H0	h	GS	DR
Trisetum spicatum	2 - 5	100	**5**	**10**	3600000	**2.00**	**5.00**	0.15	0.30	0.41	0.58	10	100	0.04	0.08	1.30	0.2	0,01	0.034	60.5
Valeriana celtica ssp. norica	2 - 5	100	1	1	1575000	2.00	5.00	0.25	0.45	0.41	0.58	10	100	0.11	0.22	1.68	0.15	0,1	0.016	50.9
Veronica alpina	2 - 5	100	**5**	**10**	1627500	**2.00**	**5.00**	0.20	0.45	0.41	0.58	10	100	0.11	0.22	1.00	0.097	0,01	0.107	71.2
Veronica aphylla	2 - 5	100	**1**	**1**	546000	**0.25**	**0.75**	0.20	0.40	0.41	0.58	10	100	0.11	0.22	1.50	0.08	0,1	0.065	64.1
Veronica bellidioides	2 - 5	100	**1**	**1**	1452500	**0.25**	**0.75**	0.20	0.40	0.41	0.58	10	100	0.11	0.22	1.52	0.2	0,1	0.068	65.0
Veronica fruticans	2 - 5	100	**10**	**10**	1050000	**2.00**	**5.00**	0.20	0.40	0.41	0.58	10	100	0.11	0.22	1.84	0.15	0,1	0.057	62.1
Viola biflora	2 - 5	100	**5**	**5**	970000	**0.25**	**0.75**	0.20	0.35	0.41	0.58	10	100	**0.14**	**0.28**	3.01	0.15	0,1	0.020	42.3

Mat – Age of maturity (minimun – maximum years); bold values from the LEDA traits database[38] other values estimated as 5–10 years for dwarf shrubs and large cushion plants (e.g. *Rhododendron spp., Salix spp., Helianthemum spp., Silene acaulis*) and 2–5 years for all others.

Age – maximum age of genets (years); set to 1 for annual species and to 100 for all clonally growing ones (= all others in the sample).

SP_l and SP_h – persistence of seeds in the soil seed bank; bold values from the IntraBioDiv project[39]; classification of other species into three categories (10 long-term persistent, 5 short-term persistent,1 transient) based on seed shape following Thompson *et al.*[40]; values of species without any seed shape information available were estimated in analogy to congeners.

CC – carrying capacity (number of individuals or shoots); we used vegetation plot data from Willner[41] to estimate maximum % cover values of the respective species under well-suited conditions and calculated the respective individual/shoot numbers by dividing the covered area by the estimated size of one individual/shoot.

CLG_l and CLG_h – low and high clonal growth rates, i.e number of offspring shoots per parent shoot; bold data were taken from the CLO-PLA database[42]; missing data were estimated in analogy to congeners or species of similar growth froms.

FF_l and FF_h – flowering frequency (% of individuals/shoots flowering per year); own estimates.

JS_l and JS_h – juvenile survival (% of individuals surviving from one year to the next); own estimates set such that the probability that a seed will establish and survive until the reproductive (adult) stage under well-suited environmental conditions and without density depedendent effects was in the order of 0.01% – 5% for low and high parameter values, respectively (see also ref. 43).

SY_l and SY_h – seed yield (number of seeds produced per flowering individual/shoot); bold data from the LEDA traits database[38] and literature[44-46] classified into three categories (1–10;10–100;100–1000); other data: own estimates.

Germ_l and Germ_h – germination rates (percentage of germinating seeds); bold data were taken from the literature[47-51]; missing data were estimated as the average germination rate (given for growth forms in Milbau *et al.*[52]) multiplied by the average survival rate of alpine seedlings in the first year[53] as high, and half of these estimates as low values, respectively.

vt – terminal falling velocity (m/s); data are averages of the values in the LEDA traits database[38]; or averages of own measurements of 20 – 50 seeds per species.

H0 – seed release height (m); taken from Fischer *et al.*[54].

h – mean height of the vegetation surrounding a fruiting plant (m), a parameter used in fitting WALD dispersal models[21,22]. Based on field experience with Alpine vegetation h was set to 0.1 m for alpine grassland plants, 0.01 m for plants of snowbed, scree and rock vegetation, and to 0.7 m for species typically occurring in tall herb communities.

GS – probability to survive the gut passage of a large mammal (fallow deer) as calculated from the seed mass by the regression equation in Mouissie[31]; seed mass data were taken from the LEDA traits database[38], supplemented by own measurements (mean of 20 – 50 seeds per species).

DR – hourly detachment rate (%) of seeds from chamois fur; assumed to be equal to the mean of the detachment rates from sheep and cattle fur as calculated from the seed mass and surface structure by the regression equations in Römermann *et al.*[28]. Seed mass data were taken from the LEDA traits database[38], supplemented by own measurements (mean of 20 – 50 seeds per species). Seed surface structure was classified from own samples (minimum n=10) of seeds of all species.

Supplementary references

(1) WorldClim – Global Climate: www.worldclim.org

(2) Hijmans, R. J., Cameron, S. E., Parra, J. L., Jones, P. G. & Jarvis, A. Very high resolution interpolated climate surfaces for global land areas. *Int. J. Climatol.* **25**, 1965–1978 (2005).

(3) Rabus, B., Eineder, M., Roth, A. & Bamler, R. The shuttle radar topography mission - a new class of digital elevation models acquired by spaceborne radar. *ISPRS J. Photogramm.* **57**, 241–262 (2003).

(4) Zimmermann, N. E., Edwards, T. C., Moisen, G. G., Frescino, T. S. & Blackard, J. A. Remote sensing-based predictors improve distribution models of rare, early successional and broadleaf tree species in Utah. *J Appl Ecol* **44**, 1057–1067 (2007).

(5) Zimmermann, N. E. *et al.* Climatic extremes improve predictions of spatial patterns of tree species. *P. Natl. Acad. Sci. USA* **106**, 19723–19728 (2009).

(6) Randin, C. F *et al.* Climate change and plant distribution: local models predict high-elevation persistence. *Global Change Biol*. **15**, 1557–1569 (2009).

(7) Engler R. *et al.* 21st century climate change threatens mountain flora unequally across Europe. *Global Change Biol*. **17**, 2330–2341 (2011).

(8) Mitchell T.D., Carter T.R., Jones P.D., Hulme M. & New, M. A comprehensive set of high-resolution grids of monthly climate for Europe and the globe: the observed record (1901-2000) and 16 scenarios (2001-2100). *Tyndall Working Paper 55*, *University of East Anglia*, Norwich (2004).

(9) Hollweg, H. D *et al.* Ensemble simulations over Europe with the regional climate model CLM forced with IPCC AR4 global scenarios. *Technical Report No. 3, Max Planck Institute for Meteorology*, Hamburg, Germany (2008).

(10) http://eusoils.jrc.ec.europa.eu, accessed 03/11/2010.

(11) Bayer, K. & Pavlik W. Databases at the Geological Survey of Austria: Substrate units in the Austrian Alps at the scale of 1:200.000. 6th European Congress on Regional Geoscientific Cartography and Information Systems (EUREGEO), Earth and Man. Proceedings Vol. 1, pp. 109-111. Landesamt für Vermessung und Geoinformation, München) (2009)

(12) Willner, W. in *Vegetation databases for the 21st century* (eds. Dengler, J. Chytrý, M., Ewald, J., Finckh, M., Jansen, F. Lopez-Gonzalez, G., Oldeland, J., Peet, R.K. & Schaminée, J.H.J. Biodiversity and Ecology 4, Hamburg) in press.

(13) Thuiller, W., Lafourcade, B., Engler, R. & Araújo, M.B. BIOMOD - A platform for ensemble forecasting of species distributions. *Ecography* **32**, 369–373 (2009).

(14) Elith, J. *et al.* Novel methods improve prediction of species' distributions from occurrence data. *Ecography* **29**, 129–151 (2006).

(15) Allouche, O., Tsoar, A. & Kadmon, A. R. Assessing the accuracy of species distribution models: prevalence, kappa and the true skill statistics (TSS). *J. Appl. Ecol.* **43**, 1223–1232 (2006).

(16) Marmion, M., Parviainen, M., Luoto, M., Heikkinen, R. K. & Thuiller W. Evaluation of consensus methods in predictive species distribution modelling. *Divers. Distrib.* **15**, 59–69 (2009).

(17) Liu, C., Berry, P. M., Dawson, T. P. & Pearson, R. G. Selecting thresholds of occurrence in the prediction of species distributions. *Ecography* **28**, 385–393 (2005).

(18) Brown, J. H. & Kodric-Brown, A. Turnover rates in insular biogeography: effect of immigration on extinction. *Ecology* **58**, 445–449 (1977).

(19) Nathan, R. Long-distance dispersal of plants. *Science* **313**, 786-788 (2006).

(20) Nathan, R., Schurr, F. M., Spiegel, O., Steinitz, O., Trahktenbrot, A. & Tsoar, A. Mechanisms of long-distance seed dispersal. *Trends Ecol. Evol.* **23**: 638–647 (2008).

(21) Katul, G.G. et al. Mechanistic analytical models for long-distance seed dispersal by wind *Am. Nat.* **166**, 368–381 (2005).

(22) Skarpaas, O. & Shea K. Dispersal patterns, dispersal mechanisms, and invasion wave speed for invasive thistles. *Am. Nat.* **170**, 421–430 (2007).

(23) Soons, M, Heil, G.M., Nathan, R. & Katul, G.G. Determinants of long-distance seed dispersal by wind in grasslands. *Ecology* **85**, 3056-3068 (2004).

(24) Morales, J. M., Haydon, D. T., Frair, J., Holsinger, K. E. & Fryxell, J.M. Extracting more out of relocation data: building movement models as mixtures of random walks. *Ecology* **85**, 2436-2445 (2004).

(25) Fankhauser, R. & Enggist, P. Simulation of alpine chamois *Rupicapra r. rupicapra* habitat use. *Ecol. Model.* **175**, 291–302 (2004).

(26) Boschi, C. & Nievergelt, B. The spatial patterns of Alpine chamois (*Rupicapra rupicapra*) and their influence on population dynamics in the Swiss National Park. *Mamm. Biol.* **68**, 16–30 (2003).

(27) Hamr, J. Home range sizes of male chamois, *Rupicapra rupicapra*, in the Tyrolean Alps, Austria. *Acta Zool. Fennica* **171**, 293–296 (1984).

(28) Römermann, C., Tackenberg, O. & Poschlod, P. How to predict attachment potential of seeds to sheep and cattle coat from simple morphological seed traits. *Oikos* **110**, 219–230 (2005).

(29) Pakeman, R. J. Plant migration rates and seed dispersal mechanisms. *J Biogeography* **28**: 795–800 (2001).

(30) Illius, A. W. & Gordon, I.J. Modelling the nutritional ecology of ungulate herbivores: evolution of body size and competitive interactions. *Oecologia* **89**, 428–434 (1992).

(31) Moussie, A.M. *Seed dispersal by large herbivores* (PhD thesis, Rijksuniversitet Groningen, 2004).

(32) Dullinger, S. *et al.* Patch configuration affects alpine plant distribution. *Ecography* **34**, 576–587 (2011).

(33) Aeschimann, P., Lauber, K., Moser, D.M. & Theurillat, J.P. *Flora Alpina. Vols. 1-3*. (Haupt Verlag, Bern, 2004).

(34) Saltelli, A., Tarantola, S, Campolongo, F. & Ratto, M. *Sensitivity analysis in practice* (John Wiley & Sons, 2004).

(35) http://simlab.jrc.ec.europa.eu/, accessed 05/10/2011.

(36) Kaplan, E. L. & Meier, P. Nonparametric estimation from incomplete observations. *Journal of the American Statistical Association* **53**, 457–481 (1958).

(37) Therneau, T. *survival: Survival analysis, including penalised likelihood*. R package version 2.36-9. http://CRAN.R-project.org/package=survival.

(38) Kleyer, M. *et al.* The LEDA Traitbase: A database of life-history traits of Northwest European flora. *J. Ecol.* **96**, 1266–1274 (2008).

(39) Gugerli, F. *et al.* Relationships among levels of biodiversity and the relevance of intraspecific diversity in conservation - a project synopsis. *Perspect. Plant Ecol., Evol. Systematics* **10**, 259–281 (2008).

(40) Thompson, K., Band, S. R. & Hodgson, J. G. Seed size and shape predict persistence in soil. *Funct. Ecol* **7**, 236–241 (1993).

(41) Willner, W. in *Vegetation databases for the 21st century* (eds. Dengler, J. Chytrý, M., Ewald, J., Finckh, M., Jansen, F. Lopez-Gonzalez, G., Oldeland, J., Peet, R.K. & Schaminée, J.H.J. Biodiversity and Ecology **4**, Hamburg) in press.

(42) Klimesova, J. & de Bello, F. CLO-PLA: the database of clonal and bud bank traits of Central European flora. *J. Veg. Sci.* **20**, 511–516 (2009).

(43) Nathan, R. *et al.* Spread of North American wind-dispersed trees in future environments. *Ecol. Letters* **14**, 211–219 (2011).

(44) Pecetti, L. *et al.* Variation in morphology and seed production of snow clover [*Trifolium pratense* L. subsp. n*ivale* (Koch) Arcang.] germplasm from the Rhaetian Alps, Italy. *Genet. Resour. Crop. Evol*. **55**, 939–947 (2008).

(45) Totland, Ø & Alatalo, J. M. Effects of temperature and date of snowmelt on growth, reproduction, and flowering phenology in the arctic/alpine herb, *Ranunculus glacialis*. *Oecologia* 133, 168–175 (2002).

(46) Miller, G. R. & Geddes C. Size and longevity of seed banks of alpine gentian (*Gentiana nivalis* L.)**.** *Botanical Journal of Scotland* **56**, 85–91 (2004).

(47) Schwienbacher, E. & Erschbamer, B. Longevity of seeds in a glacier foreland of the Central Alps – a burial experiment. *Bull. Geobot. Inst. ETH* **68**, 63–71 (2001).

(48) Weppler, T., Stoll, P. & Stöcklin, J. The relative importance of sexual and clonal reproduction for population growth in the long-lived alpine plant *Geum reptans. J. Ecol.* **94**, 869–879 (2006).

(49) Evju, M., Halvorsen, R., Rydgren, K., Austrheim, G. & Mysterud, A. Interactions between local climate and razing determine the population dynamics of the small herb *Viola biflora. Oecologia* **163**, 921–933 (2010).

(50) Schwienbacher, E., Marcante, S. & Erschbamer, B. Alpine species seed longevity in the soil in relation to seed size and shape. A 5-year burial experiment in the Central Alps. *Flora* **205**, 19–25 (2010).

(51) Dullinger S. & Hülber K. Experimental evaluation of seed limitation in alpine snowbed plants. *PLoS ONE* **6**, e21537 (2011).

(52) Milbau, A., Graae, B. J., Shevtsova, A. & Nijs, I. Effects of a warmer climate on seed germination in the subarctic. *Ann. Bot*. **104**, 287–296 (2009).

(53) Forbis, T. A. Seedling demography in an alpine ecosystem. *Am. J. Bot.* **90**, 1197–1206 (2003).

(54) Fischer, M.A., Oswald, K. & Adler, W. *Exkursionsflora für Österreich, Liechtenstein, Südtirol*. 3rd edn. Linz, Biologiezentrum des Österreichischen Landesmuseums (2008).